JOURNAL OF MATERIALS SCIENCE 25 (1990) 343–352

Investigation of the reduction kinetics of wustite fine powders

P. G. COOMBS, Z. A. MUNIR
Division of Materials Science and Engineering, University of California, Davis, California 95616, USA

The reduction of wustite (FeO) by hydrogen was investigated over the temperature range 723 to 873 K. The reduction mechanism was found to depend on temperature relative to an effective eutectoid decomposition temperature of 803 K. Above this temperature the reaction proceeds directly according to: $FeO + H_2 = Fe + H_2O$ while below this temperature the reduction is accomplished through the following two sequential steps: $4FeO = Fe + Fe_3O_4$ and $Fe + Fe_3O_4 + 4H_2 = 4Fe + 4H_2O$. Approximate activation energies for reduction above and below 803 K were determined to be 51 and 58 kJ mol^{-1}, respectively. Investigations were also conducted on the oxidation of the iron resulting from the reduction of FeO.

1. Introduction

Wustite, a metal deficient oxide with a nominal formula of FeO is thermodynamically stable at relatively high temperatures and under a low partial pressure of oxygen. It undergoes a eutectoid decomposition at 843 K producing α-iron and another oxide, magnetite. At this temperature, wustite is stable only in the presence of $P_{O_2} < 10^{-26}$ atm [1]. Although thermodynamic stipulations exclude the presence of wustite below the eutectoid temperature (843 K), there is experimental evidence that this oxide can exist in thin film form at temperatures at least 150 K below the eutectoid isotherm [2].

Previous investigations on the reduction of FeO have utilized samples in the form of thick [3] and thin foils [4], and in the form of powder with relatively large particles (170 μm) in a fluidized bed [5]. The reduction of dense crystals of FeO was also investigated [6].

In this work we report the results of an investigation on the hydrogen reduction of sub-micrometre sized particles of FeO in the temperature range 723 to 873 K. We also report the results of the subsequent oxidation of the reduction product, iron. This investigation is part of a larger study on the role of sintering on oxidation–reduction and dissociation reactions [7–10]. In a subsequent paper [11] we report the results of similar studies on Fe_2O_3.

2. Experimental materials and methods

Iron oxide (FeO) powders, reported to be 99.8% pure, were purchased from the Atomergic Co., New York. Spectroscopic analysis conducted independently on the wustite sample showed it to contain silicon as the major impurity (at a level of 0.4 wt %). Other identified impurities included manganese (0.08 wt %), aluminium (0.07 wt %), and zinc (0.05 wt %). A variety of other metallic elements was also identified but their levels were typically $\leqslant 0.02$ wt %. The level of all impurities as determined by the spectroscopic analysis (0.7 wt %) exceeds the 0.2 wt % stated by the supplier by more than a factor of three. A particle size distribution of the powder showed the most probable particle size to be about 0.25 μm. However, in view of a surface area analysis which gave a value of 0.286 m^2 g^{-1}, it is concluded that the powder is highly agglomerated.

The sample size used in all experiments was 150.00 mg. This quantity was placed in a cylindrical alumina crucible with a diameter of 3.3 cm. Reduction of FeO was carried out in a continuous recording microbalance (Cahn Model 1000) under 1 atm flowing hydrogen gas. Experiments were carried at 723, 773, 823, and 873 K with a hydrogen flow of 30 ml min^{-1}. A much higher hydrogen flow level (430 ml min^{-1}) gave rise to crucible oscillations and hence to uncertainties in the weight change data. After the oxide samples were placed in the reaction tube and the tube evacuated, the system was back-filled to a pressure of 1 atm using 99.998% purity argon gas. Following this, the system was again evacuated to a pressure less than 27 MPa (2×10^{-4} torr). This sequence of evacuation, back-filling, and re-evacuation ensured the elimination of gaseous contamination in the reaction system. Finally, the system was filled to 1 atm with hydrogen gas. The 99.99% pure hydrogen was passed through a drierite tube, a 0.5 nm molecular sieve, and a P_2O_5 drying agent before entering the reaction tube. Once the system had been brought up to 1 atm with hydrogen, the gas outlet from the system was opened and a hydrogen flow rate of approximately 30 ml min^{-1} was established. This flow rate was maintained throughout the reduction experiments. The stream of hydrogen entered the reaction tube through the bottom and exited through a side tube and a bubbler attached to the top of the reaction tube.

In all reductions, the samples were heated to the desired temperature at 10 K min^{-1} using a programmable temperature controller. For the FeO

0022–2461/90 $03.00 + .12

samples, reduction temperatures of 723, 773, 823, and 873 K were used. Once the temperature had reached its set value, it was held there until the prescribed reaction time had passed. The reduction was then stopped by the cooling of the sample and reaction tube. To speed cooling, the insulating flaps at the top and bottom of the furnace were opened. Typically, the sample cooled down to 423 K (150° C) in ~30 min. The hydrogen flow was maintained throughout the cool-down period. The durations of the FeO reductions generally differed from one experiment to the next due to the unusual nature of the reduction's temperature dependence, as will be seen later.

The oxidation of the product of FeO reduction was also investigated in this study. All oxidations were carried out in air at 1 atm. Following the reduction process, the chamber was first evacuated to a pressure less than 27 mPa (2×10^{-4} torr). The chamber was then back-filled to 1 atm with argon gas and re-evacuated to 27 mPa. Finally, the system was brought up to 1 atm with dried room air, and the temperature was increased at a rate of 10 K min^{-1}.

The duration of the oxidation experiments varied with some oxidations being as short as 5.5 h while others were as long as 36 h. Four temperatures were used in the oxidation experiments: 723, 823, 873 and 898 K.

3. Results

3.1. Reduction of FeO

As stated earlier, the FeO samples were heated to the specified reduction temperature at a constant rate of 10 K min^{-1}. The weight of the sample remained constant until the temperature reached approximately 615 K. At this and higher temperatures, the weight of the sample began to fall, signalling the start of the reduction process. The time at which this occurred was defined as time zero for calculation purposes, and all reduction curves start at this point. Given enough time, FeO samples could be fully reduced at any of the four selected temperatures with an accompanying weight loss of 33.79 mg. This compares very well to the theoretical weight loss of 33.40 mg (based on a starting FeO weight of 150.00 mg). However, the temperature dependence of the reduction process was found to be contrary to general expectations. As expected, reductions at 773 were faster than reductions at 723 K, and similarly reductions at 873 K were faster than those at 823 K. However, reductions at 823 and 873 K were actually slower than those at the lower corresponding temperatures (see Fig. 1). As can be seen in the figure, at 723 K the reduction was complete after only 1.5 h. At 823 K, however, some oxide remained even after 5.0 h. Increasing the temperature from 823 to 873 K speed up the reaction, but the reduction rates for time after 1.0 h were still very low.

The critical temperature at which the rate of reduction changed was determined to be approximately 803 K. Test experiments were carried out in which the temperature was varied around this critical point and the accompanying changes in the reduction behaviour observed. The results of one of these experiments are displayed in Fig. 2. Referring to this figure, the reduction was first carried out at 723 K, and when the sample weight had reached an approximate value of 22 mg (point a in the figure), the temperature was increased towards 823 K at a rate of 10 K min^{-1}. The reduction rate increased initially, but when the temperature reached 798 K, the rate decreased discontinuously. The point at which this occurred can be seen to correspond with the weight of 16 mg (point b, Fig. 2). The temperature continued to increase, and reached the upper limit of 823 K before the sample weight decreased to 15 mg. At a weight equal to 12.5 mg (point c), the furnace power was turned down. The temperature had dropped to 779 K at the point on the curve with weight 10 mg (point d). At this time, the slope increased again discontinuously. Beyond the

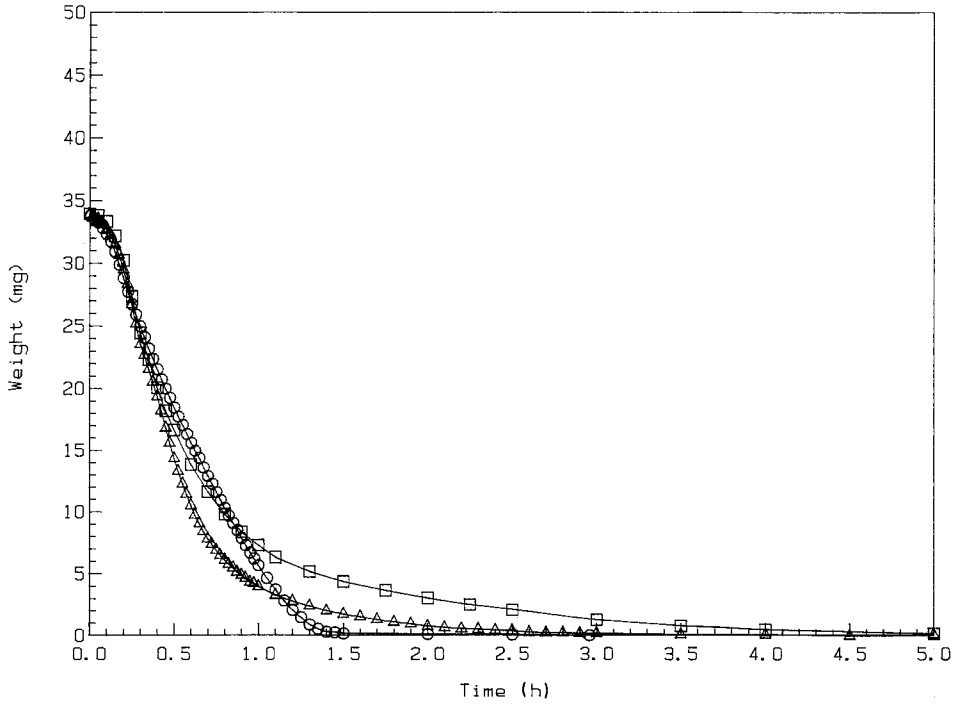

Figure 1 The temperature dependence of the hydrogen reduction of wustite powders. Reduction at (○) 723 K, (□) 823 K, (△) 873 K.

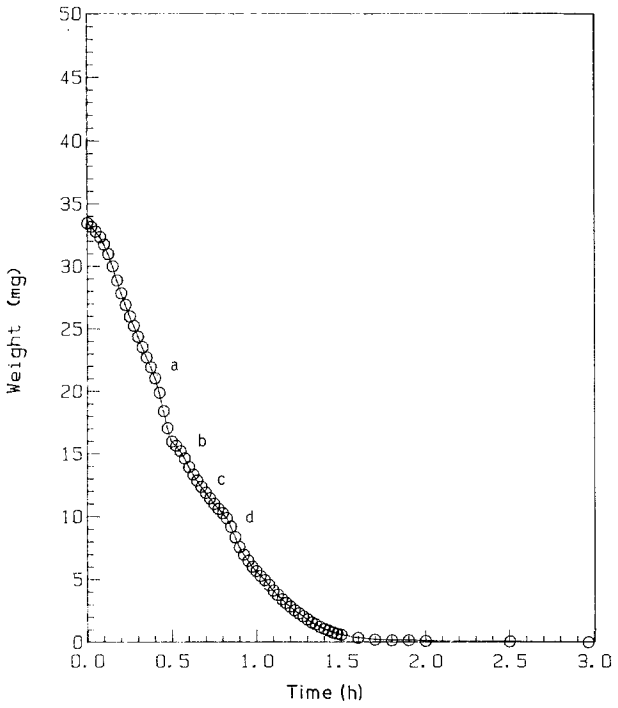

Figure 2 Effect of temperature variation during the reduction of FeO. (○) 723/823/723 K reduction.

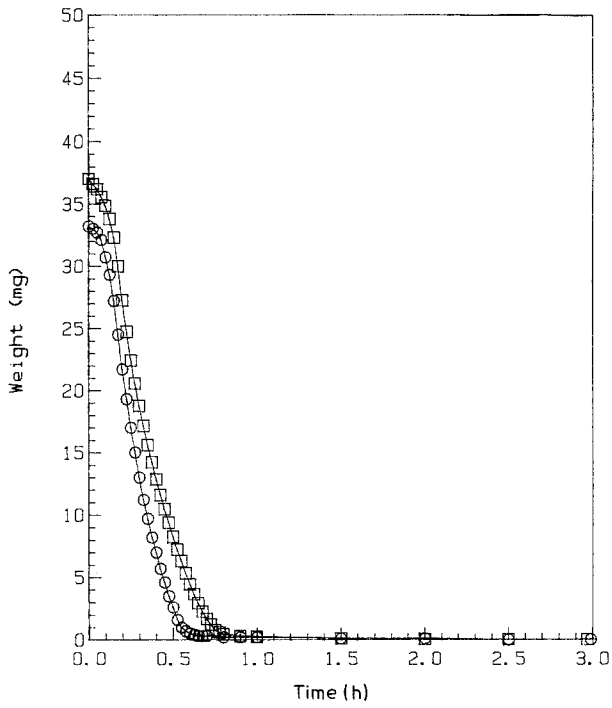

Figure 4 The effect of the degree of oxidation on the subsequent reduction of iron oxide samples: (○) after 9 h, (□) after 24 h. T = 723 K.

second slope change, the slope decreased until it reached a zero value at the end of the experiment, as seen in Fig. 2. The slope in the final portion of the test experiment was lower than at equivalent points in the normal experiment at 723 K as can be seen by comparing Figs 1 and 2.

Following the first reduction to iron, many samples were re-oxidized in air. As will be discussed later, the re-oxidation led to the formation of Fe_3O_4 and Fe_2O_3 instead of FeO, as expected under the prevailing experimental conditions. When these incompletely oxidized samples were reduced a second time, the reductions were faster than before. In every instance, the second reduction was considerably faster than the first. Fig. 3 shows the typical first and second reduction behaviour of the (initially) FeO samples at 723 K. In this graph, the second reduction can be seen to take place in approximately half the time of the first reduction. It should be pointed out that the start of the two curves at approximately the same weight is a coincidence. The samples do not start out as the same oxide but happen to contain the same amount of oxygen.

The rates of the second reductions were not found to be functions of the amount of oxide formed during the first oxidations. Fig. 4 shows the results of two different second reductions. One of the samples had been oxidized for a longer period of time prior to reduction, and hence contained approximately 37 mg oxygen compared to 33 mg for the other sample. The shapes of the two curves are virtually identical, implying no dependence on the degree of oxidation.

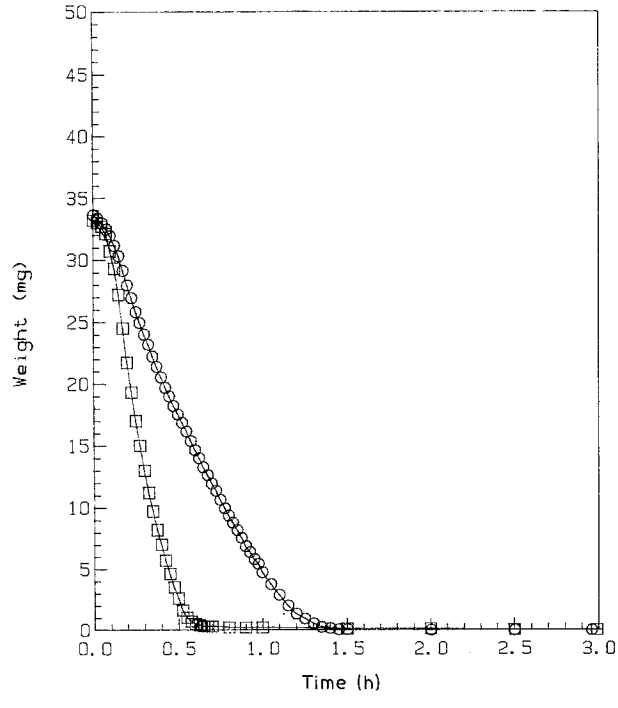

Figure 3 The effect of cycling on the reduction of FeO. (○) First reduction, (□) second reduction. T = 723 K.

3.1.1. Reduction kinetics

At temperatures below the observed critical point (803 K), the reduction of FeO produced curves of weight against time with sigmoidal shapes. This was the same behaviour as that observed by El-Rahaiby and Rao [4] in their study on the hydrogen reduction of thin foils of FeO at temperatures between 511 and 690 K. These authors analysed the kinetics of FeO reduction by assuming a zero-order rate relation and determining the rates of reduction at various temperatures in the steady-state portions of the sigmoidal curves.

The kinetic equation for a linear rate can be expressed mathematically as

$$r = \mathrm{d}(\Delta W)/\mathrm{d}t \qquad (1)$$

where r is the rate of reduction of the oxide, ΔW the weight loss of the sample (mg), t the time (min). The

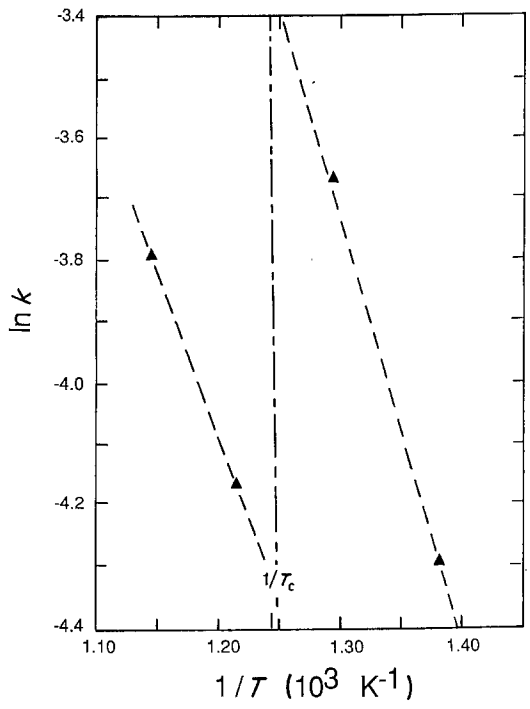

Figure 5 The temperature dependence of the rate constant of the reduction of FeO.

rate constant can be defined as

$$k = r/\Delta W_t \quad (2)$$

where ΔW_t is the maximum (theoretical) weight loss. The slopes in the steady-state regions of the reduction curves were calculated at the four experimental reduction temperatures. Unfortunately, at 823 K the steady-state slope was difficult to determine due to the shape of the curve (see Fig. 1). In this case, the slope at the mid-point of reduction was determined and used in further calculations. The values obtained for the rate constant using Equation 2 are listed in Table I and plotted in Fig. 5. Above and below the observed

TABLE I Rate constants for the reduction of FeO powders in hydrogen

T (K)	k (10^{-2} min^{-1})
723	1.36
773	2.55
823	1.55
873	2.25

critical temperature of 803 K, the rate constants show a significant shift in value. The reason for the discontinuity and its relationship to the critical temperature will be discussed in a later section of this paper. However, approximate activation energies were calculated from the temperature dependences of the rate constant values over the two temperature regions. The low- and high-temperature activation energies for wustite reduction were determined to be 58 and 51 kJ mol^{-1}, respectively.

3.2. Oxidation of iron produced by the reduction of FeO

3.2.1. Oxidation behaviour

The oxidation behaviour of iron reduced from FeO depended strongly on temperature and the cycling history. Samples were oxidized through one or two complete reduction–oxidation cycles. As was noted before, the second reductions were faster than the first. Similar observations were made in the case of oxidation. Fig. 6 shows the oxidation results for a sample reduced and oxidized twice at 723 K. Initially, the oxidation rates were very high; however, after only about 0.5 h, the rate decreased dramatically and continued to decrease throughout the rest of the experiment. In the initial stages of the two oxidations ($t < 0.25$ h), shown in Fig. 6, the rate started at a high level, and then increased further. In fact, the second oxidation curve is almost vertical between weight levels of 10 and 17 mg.

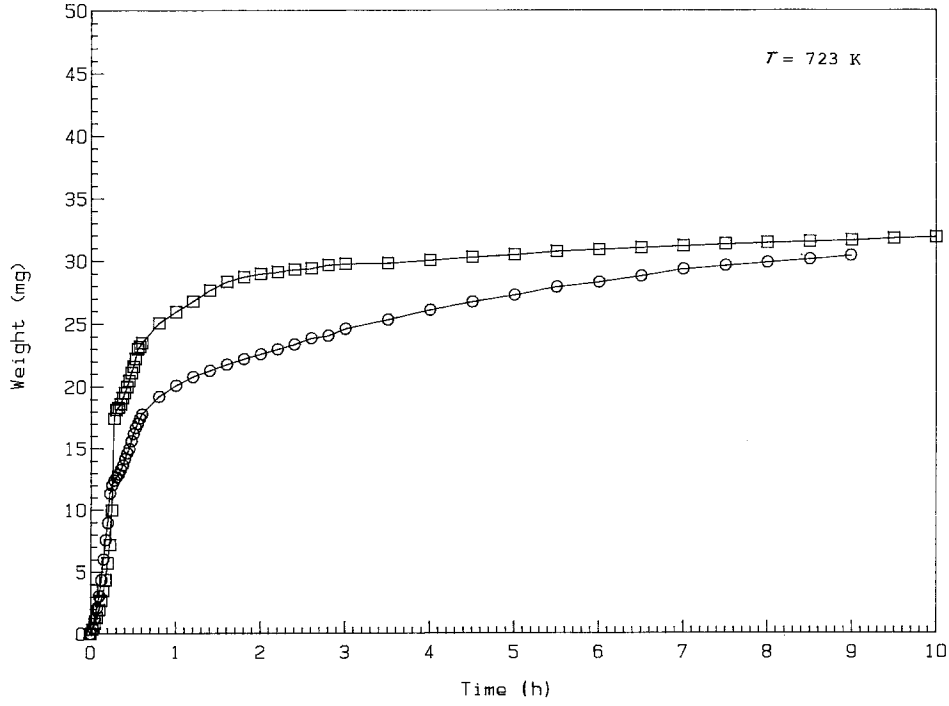

Figure 6 The effect of cycling on the oxidation of iron produced by the reduction of FeO. (○) First oxidation, (□) second oxidation.

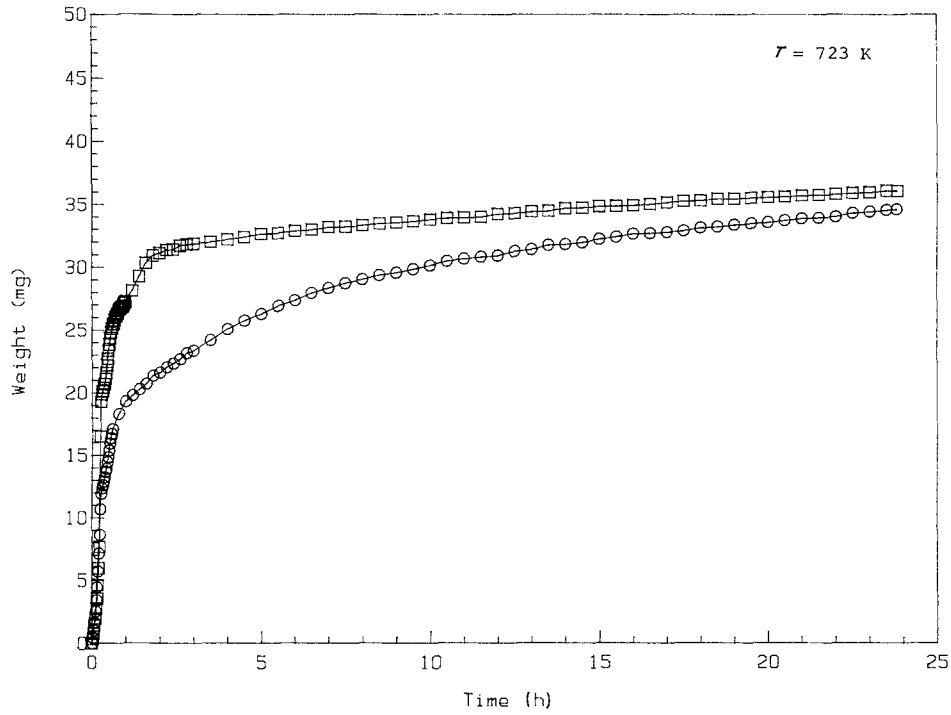

Figure 7 Extended oxidation of products of reduction of FeO. (○) First oxidation, (□) second oxidation.

To fully oxidize the iron to Fe_2O_3, the samples would have to have gained 50 mg. This degree of oxidation was not even approached at 723 K. At this temperature, the two oxidation curves appear to be asymptotically approaching a weight value of only about 31 mg, or 63% oxidation. Even when the oxidation is carried out for 24 h, Fig. 7, the total weight gain was only 36 mg, or about 72% conversion to Fe_2O_3.

A comparison between the oxidation behaviour at 723 K and that at 873 K is shown in Fig. 8. At 873 K, the sample was over 92% oxidized after only 9 h. These two samples, however, have different thermal histories. The 723 K sample had been reduced at 723 K, while the 873 K sample had been reduced at 873 K, which took longer to reach completion. The two oxidation curves in Fig. 8 appear as one line during the early stages of oxidation.

Although the emphasis in the present work is on the reduction process of FeO, an attempt was made to determine the reaction kinetics of the iron samples resulting from the reduction process. It has been reported that sheets or foils of iron normally oxidize with a parabolic rate relation [12]. Such an oxidation mode was not observed in the present study. In fact, following the initial, high-rate region, the rate

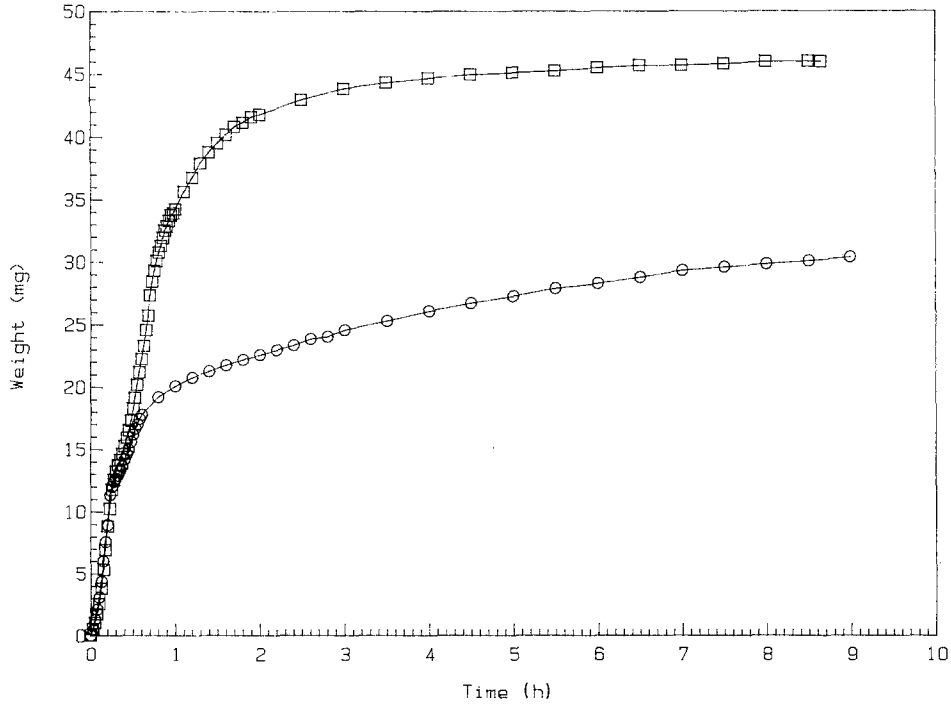

Figure 8 The temperature dependence of the first oxidation of iron produced by the reduction of FeO. Oxidation at (○) 723 K, (□) 873 K.

TABLE II X-ray diffraction results for FeO samples exposed to varying temperature and cycling conditions*

(a) Cyclic reduction–oxidation

T (K)	Sample	Thermal history	Compounds detected
723	BB	1R 1OX	Fe_3O_4, Fe_2O_3, FeO, possibly Fe
723	BA	2R 2OX	Fe_3O_4, Fe, Fe_2O_3, FeO
723	AF	2R 2OX	Fe_3O_4, Fe_2O_3, possibly Fe
723	AJ	2R 2OX	Fe_3O_4, Fe, Fe_2O_3
723	BC	2R 2OX (24 h)	Fe_3O_4, Fe_2O_3
823	AC	1R 1OX	Fe_2O_3
873	AK	1R 1OX	Fe_2O_3, possibly Fe_3O_4
723/898	AD	1R at 723 1OX at 898 (rapid heating)	Fe_2O_3
823/898	AE	1R at 823 1OX at 898 (incomplete reduction; rapid heating in CO_2)	Fe_3O_4

(b) Partial reductions

T (K)	Sample	Per cent reduction	Compounds detected
723	AT	23	FeO, Fe, Fe_3O_4
723	AV	81	Fe, FeO, possibly Fe_3O_4
723	AR	95	Fe, FeO
823	AG	75	Fe, FeO, possibly Fe_3O_4
873	AW	90	Fe, FeO
873	AQ	95	(not measured)
903/873	AU	72	Fe, Fe_3O_4, FeO

(c) Other experiments

Sample	Thermal history	Compounds detected
AX	Run in argon at 723 K	Fe_3O_4, FeO, Fe
AY	Ramped to 598 K, cooled immediately	FeO, Fe, Fe_3O_4
AZ	Ramped to 598 K, held at 553 K	FeO, Fe, Fe_3O_4

*R and OX refer to reduction and oxidation cycles, thus 1R 1OX signifies one reduction and one oxidation cycle, etc.

decreased so quickly that even a cubic rate law could not represent the data.

3.3. Phase analysis

The product of reduction of FeO samples was identified by X-ray methods as iron only. However, the product of oxidation of the resulting iron depended on the thermal history. As was indicated above, the iron produced by the reduction of FeO did not fully oxidize to Fe_2O_3, and that in most instances the conversion was far from complete. A summary of the cycling histories and X-ray diffraction results is given in Table II. The observed phases are listed in decreasing order of concentration.

At 723 K, Fe_3O_4 was the primary oxide formed in every sample, regardless of whether the sample was cycled once (one oxidation and one reduction) or twice. Although Fe_2O_3 was also found, it was present in smaller concentrations. Relatively large amounts of unreacted iron were detected in samples cycled twice. In contrast, in the sample cycled once, only a possible trace of iron could be detected. In two of the five 723 K samples, small amounts of FeO were detected. This observation is unexpected because the materials were fully reduced before oxidation and the temperature of oxidation is well below the lower limit of stability of FeO.

At the two highest temperatures, 823 and 873 K, the samples gained enough weight in the first oxidation to account for at least 90% conversion to Fe_2O_3. In the sample cycled once at 823 K, Fe_2O_3 was the only compound detected, while in the sample cycled once at 873 K, possible trace amounts of Fe_3O_4 were also present. Two other samples were cycled once, but had different reduction and oxidation temperatures. The first sample was reduced at 723 K and then oxidized at 898 K at a heating rate of about 20 K min^{-1}. It was hoped that if the temperature was increased fast enough, the stability region of FeO could be reached before significant oxidation had occurred. This was not possible, however, and Fe_2O_3 was the only oxide detected after the 7 h oxidation. Another test experiment was carried out in which the oxidation took place in an atmosphere of high-purity carbon dioxide instead of air. The same rapid heating rate was employed. In this case, Fe_3O_4 was also the only oxide detected after 8.5 h at 898 K.

As stated earlier, iron was the only material detected in completely reduced samples. Analyses were also made on partially reduced samples in the hope of determining the cause of the unusual temperature dependence in the reduction of FeO (see Fig. 1). The results of these experiments, as well as the results of other related experiments, are given in Table II. A sample reduced 90% at 873 K (within wustite's stability region) contained a majority of iron, and a small amount of unreduced wustite. Another sample reduced 75% at 823 K, a temperature below the lower limit of stability of FeO but above the critical temperature observed in this study, was made up of iron and FeO,

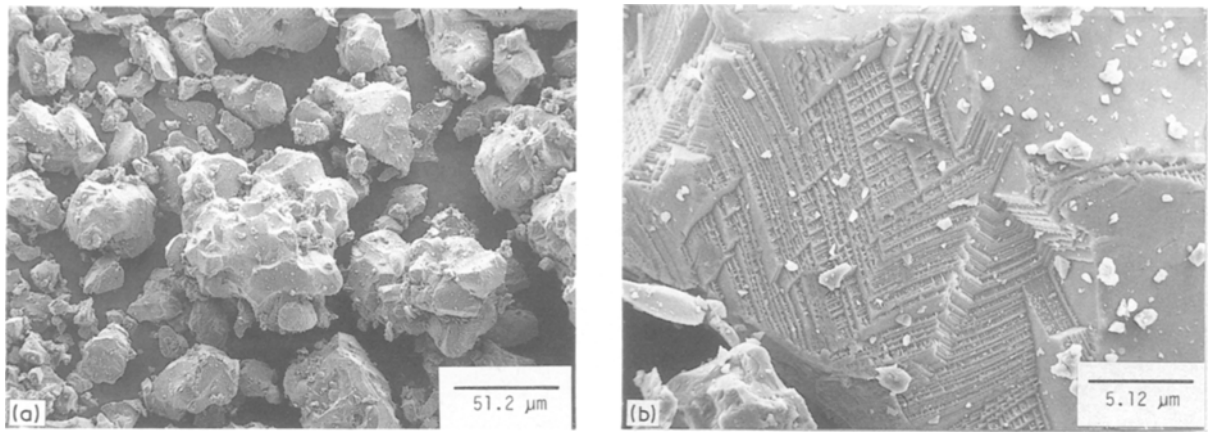

Figure 9 (a) Scanning electron micrograph of the as-received FeO powder. (b) Morphological features on the as-received FeO powder.

with a possible trace of Fe_3O_4. At the lowest reduction temperature (723 K), Fe_3O_4 was detected in partially reduced FeO samples. The largest amount of Fe_3O_4 was found in the sample reduced only 23%. A trace amount of Fe_3O_4 was found after an 81% reduction, and no Fe_3O_4 was found after a 95% reduction. In these three samples, iron and FeO were the other materials detected.

The presence of Fe_3O_4 in partially reduced FeO samples is an indication of the eutectoid decomposition of FeO to iron and Fe_3O_4. Additional experiments were made to gain a qualitative understanding of this decomposition. The first experiment was carried out in a flow of argon gas at 723 K. After 3.5 h, the sample was cooled in the same manner as the reduction experiments and removed for diffraction analysis. The analysis showed the sample to contain a majority of Fe_3O_4 and lesser amounts of FeO and iron (see Table II). Two other test runs were made in hydrogen. In the first, the sample was heated to 598 K, which is just below the temperature at which reduction usually began, and then cooled immediately to room temperature. In the second experiment, the sample was again heated to 598 K, but was then cooled to 553 K and held at that lower temperature for 3.5 h. Both samples contained at least some Fe_3O_4. The sample held at temperature contained more Fe_3O_4 than the sample which was cooled immediately.

3.4. Scanning electron microscopy

Six different samples, whose histories represented key points in the reduction and oxidation of FeO, were examined using a scanning electron microscope (SEM). The as-received material was found to contain not only a majority of small particles (as indicated by the optical image analysis), but also a substantial number of larger particles. Fig. 9a reveals the shape of the larger particles and the agglomeration of the smaller particles on the larger ones. Close up views of the particles themselves show them to be generally smooth with no apparent surface layer. Many angular features resembling etch pits were evident, however (see Fig. 9b).

If no shrinkage occurs, the reduction of FeO should leave an iron sample with approximately 44% porosity. Fig. 10a demonstrates the very porous structure left behind following reduction in hydrogen. In addition to pores, cracks were observed often in fully reduced particles. The overall shape of the particles remained constant during the first reduction, and in fact, remnants of the original surface features were even visible (see Fig. 10). No obvious signs of sintering, such as neck growth or rounded particle edges, were seen in the micrographs.

SEM analysis of two partially reduced samples added more information to that gathered through X-ray analysis. Fig. 10b demonstrates the iron growth process in action for a sample reduced 23% at 723 K. For example, in the left-hand and right-hand portions of Fig. 10b (denoted a), the surface is smooth and relatively unreacted. In the centre (region b), however, the pores and cracks indicate that reduction of the

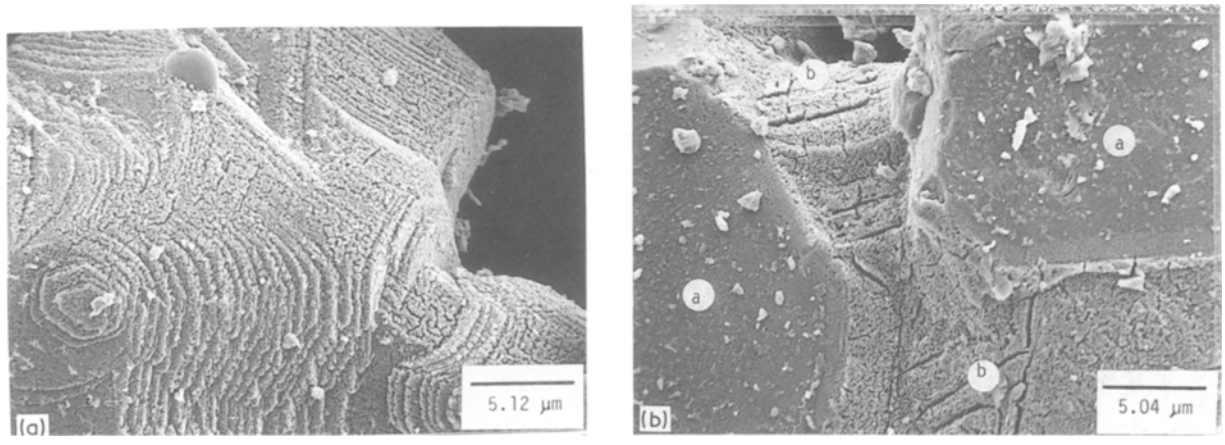

Figure 10 (a) The porous structure of fully reduced FeO (773 K in H_2 gas). (b) The structure of partially (23%) reduced FeO (723 K).

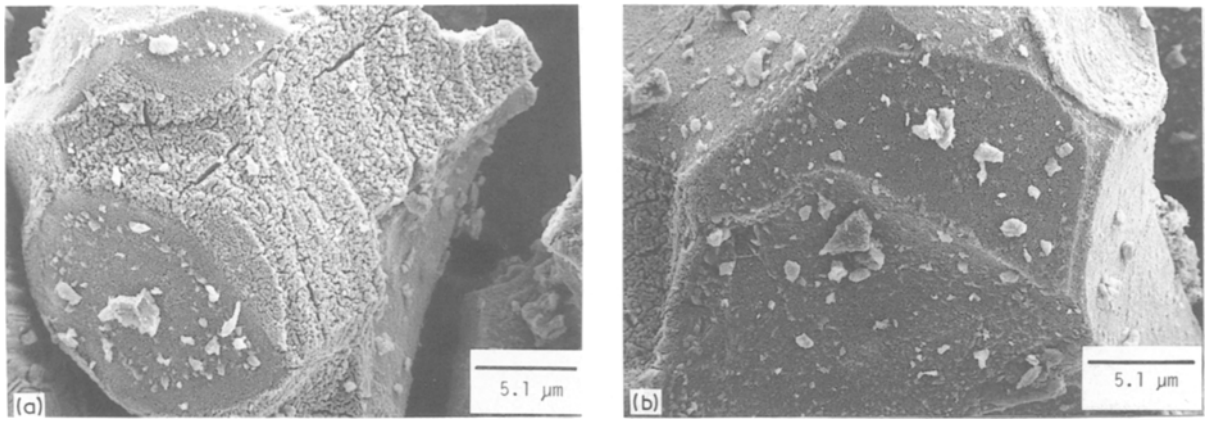

Figure 11 (a) The structure of 81% reduced FeO: mostly reacted region (723 K). (b) The structure of 81% reduced FeO: mostly unreacted region (723 K).

oxide has already occurred. Visual analysis of the areas seen in Fig. 10b as well as other areas in the sample showed the iron phase nucleating at surface discontinuities and growing out into the rest of the particles. A micrograph of a sample which had been reduced 81% at 723 K is shown in Fig. 11a. The structure of the particles looked very much the same as those in the lesser reduced sample, but the fraction of porous particles was now greater. Some particles could still be found, however, which appeared largely unreacted (see Fig. 11b).

SEM observations were also made on partially oxidized samples. A sample which was oxidized 92% at 873 K was composed almost entirely of Fe_2O_3. The most striking difference between the oxidized material and the reduced material is the "fuzziness" of the particles (see Fig. 12a). Long hair-like growths protruded from the outer surface of most of the particles. The protrusions themselves can be seen in much greater detail in Fig. 12b. Another SEM observation was made on a sample which had been cycled twice, but was oxidized to a much lower level, only 72%. It was composed of Fe_3O_4 and Fe_2O_3, with more of the former than the latter. The coarse appearance of the particles was much the same as in the previous sample, but the out-growths were much shorter (see Fig. 13a). Close up views of the protrusions revealed that they resembled vanes more than hairs (see Fig. 13b). These vanes are less prevalent in exposed areas such as humps (region c, Fig. 13b) than they are in more protected areas (region d).

Although not obvious in the reduced iron samples, some signs of sintering were visible in the partially oxidized samples. While the degree of sintering was difficult to ascertain due to the surface growths which obscure surface detail, careful examination of Figs 12 and 13 disclosed regions of neck growth and particle-to-particle bonding (denoted on the figures by e).

4. Discussion

4.1. FeO reduction behaviour

The reduction behaviour of wustite powder was found to be highly dependent not only on the absolute temperature, but also on the temperature relative to a critical value of 803 K observed in this study. Below 803 K, the reduction progressed smoothly with near-constant rates from beginning to end. Above this temperature, however, the sample weight approached its final value asymptotically. It is proposed here that 803 K is the effective eutectoid decomposition temperature for wustite under the conditions employed in this study. This temperature is 40 K lower than the reported equilibrium eutectoid temperature of 843 K [1]. As indicated earlier, however, thin films of FeO on iron have been reported at temperatures as low as 673 K [2].

We suggest, therefore, that at the two highest experimental temperatures (823 and 873 K) the

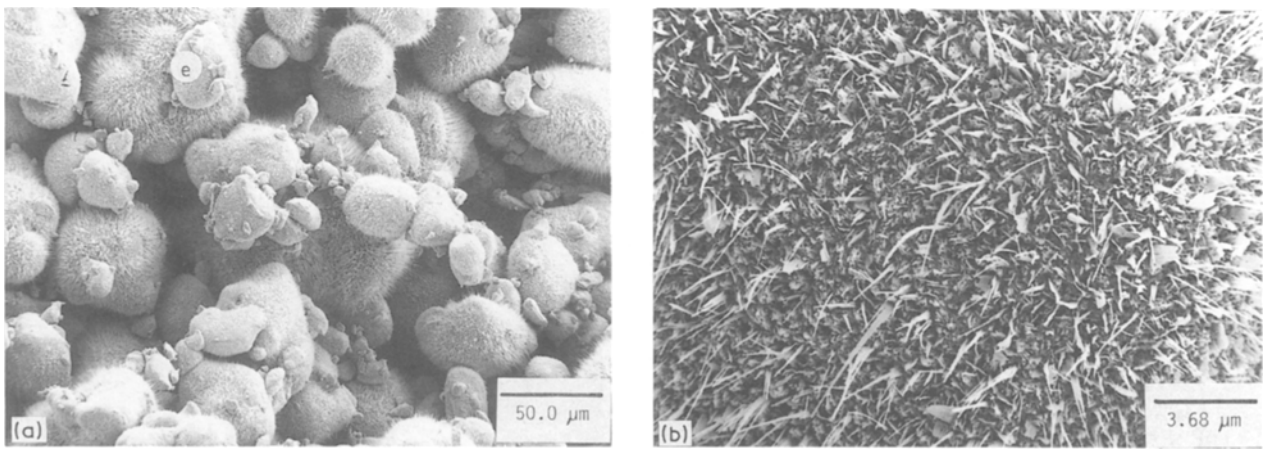

Figure 12 (a) Scanning electron micrograph of iron oxidized at 873 K for 9 h. (b) Close-up view of hair-like appearance of sample shown in (a).

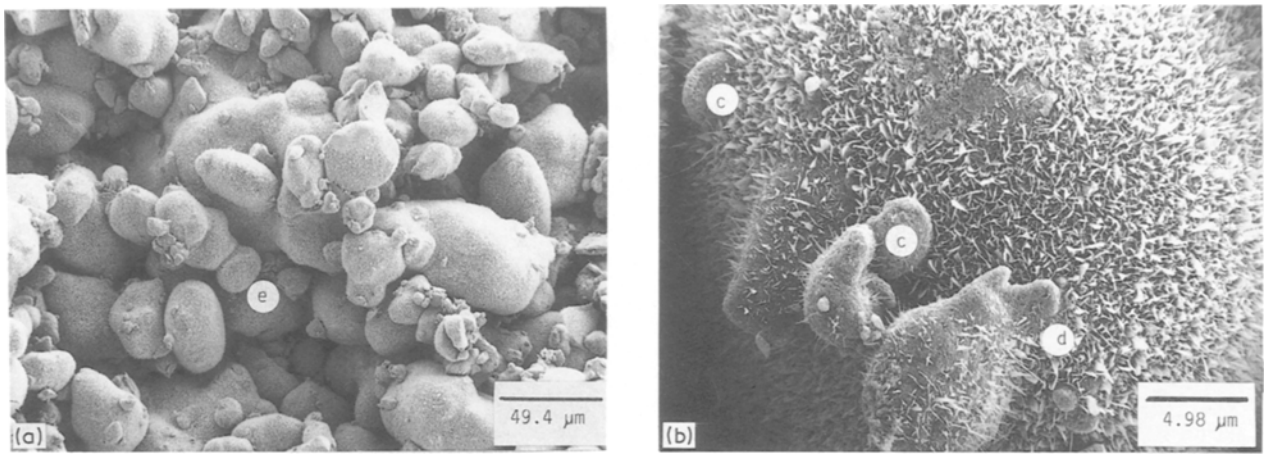

Figure 13 (a) Scanning electron micrograph of iron oxidized at 723 K for 24 h. (b) Vane-like growth on sample shown in (a).

reduction of wustite follows the reaction

$$Fe_{1-x}O + H_2 \rightarrow (1 - x)Fe + H_2O \quad (3)$$

At the two lowest temperatures (723 and 773 K), however, the reduction of oxide is preceded by the eutectoid decomposition of wustite to iron and Fe_3O_4, i.e.

$$Fe_{1-x}O \rightarrow (0.25 - x)Fe + 0.25\ Fe_3O_4 \quad (4)$$

This overall reduction of the wustite at 723 and 773 K is believed to be dominated by the Fe_3O_4 reduction, not the direct FeO to iron reduction. An extrapolation of the reduction rates from the high-temperature region (see Fig. 5) to 773 K gave a reduction rate of 18.3 mg h^{-1}. The actual value measured at this temperature was 51.1 mg h^{-1}, almost three times higher than the predicted direct reduction contribution. Thus in accordance with the proposed mechanism, the presence of the products of the eutectoid decomposition accelerates the reduction process.

The effect of the eutectoid decomposition on the reduction kinetics of FeO has been previously studied by El-Rahaiby and Rao [4]. They examined the reduction of thin foils of FeO that were (a) fully transformed to iron and Fe_3O_4 prior to reduction, (b) quenched from the oxidation temperature to avoid decomposition, and (c) partially transformed by slow cooling from the oxidation temperature. They found that in the temperature range 511 to 690 K, the fully transformed specimens reduced in about 60% of the time required for the quenched samples. Interestingly enough, the partially transformed samples had reduction kinetics very similar to the quenched samples [4]. They theorized that the reduction of wustite was controlled by a nucleation and growth process of iron in the FeO matrix. Eutectoid decomposition was thought to accelerate the reduction of FeO by producing a dispersion of iron nucleation sites. This contention was supported by micrographs which showed voids distributed throughout the iron matrix instead of concentrated at the grain boundaries of the thin foil specimens [4]. Interestingly, the micrographs of their fully transformed and reduced specimens look very much like the photographs in Fig. 10 which are for samples reduced here at 723 K, i.e. in the region in which reduction is preceded by the eutectoid decomposition.

With a nucleation and growth mechanism for wustite reduction, the eutectoid decomposition of FeO to iron and Fe_3O_4 can increase the reduction rate in two ways: the iron centres created in the decomposition can decrease the incubation time normally associated with nucleation; and the Fe_3O_4 formed in the decomposition will reduce faster than FeO. This second proposal is supported by reduction results for samples reduced and oxidized twice. At 723 K, the first oxidation produced a partially oxidized sample which was almost entirely composed of Fe_3O_4. The reduction which followed had a rate approximately twice that of the first (FeO) reduction (see Fig. 3). If Fe_3O_4 reduced to iron faster than FeO, it would be expected that Fe_3O_4 would be preferentially reduced. This prediction was substantiated by the results of the partial reduction experiments. At 723 K, the amount of Fe_3O_4 detected in the samples decreased with increasing degree of reduction. In the sample reduced 95%, FeO was still detectable even though no Fe_3O_4 was observed (see Table II).

4.2. Reduction kinetics

Zero order, or linear, kinetics describe adequately the observed weight loss data in the wustite reduction experiments. The slope did not stay constant for very long at 823 K, however, as stated in Section 3. The rate constants calculated from the slopes were plotted in Fig. 5 in an Arrhenius manner. In examining this figure, it appears that the eutectoid decomposition effectively shifts the line connecting the rate constants while not significantly changing its slope. This is reflected in the values of the reduction activation energies. The activation energies for the low- and high-temperature regions were 58 and 51 kJ mol^{-1}, respectively. Because there were only two experimental points available for each region, the calculated activation energies can only be considered approximate in nature. El-Rahaiby and Rao [4] reported a value of 71.55 kJ mol^{-1} in their investigation of thin foil reduction at temperatures between 511 and 690 K. In the higher temperature range (823 to 873 K), the activation energy determined in the present study (51 kJ mol^{-1}) compares well with the value of 59.4 kJ mol^{-1} reported by Sasabe *et al.* [6] for the reduction of dense FeO crystals between 873 and 1273 K.

4.3. Oxidation of iron produced by the reduction of FeO

Two findings in the experiments of iron oxidation are of particular interest. The first is the lack of correlation between the observed behaviour and reported expressions for the oxidation kinetics. Normally, iron samples would be expected to oxidize with a parabolic rate relation at elevated temperatures [12]. Furthermore, given enough time at high temperatures, the sample would be expected to oxidize completely to Fe_2O_3 [12]. In the oxidations carried out in this part of the study, however, the oxidation process took place with extremely high rates initially, then slowed dramatically after a few hours (see Fig. 6). The scanning electron micrographs revealed that during reduction, the wustite particles retained their original shape but became very porous. In the initial stages of oxidation, therefore, it is likely that the oxide would form in the interior of the porous iron particles as long as oxygen could penetrate inside.

As was seen earlier, the second oxidations took place at faster rates than the first oxidations. If the particles remained the same size during the first oxidation, the sample would gain only 21.7 mg, and because a 30 mg weight gain was not unusual during the first oxidations, at least some of the oxide must have grown beyond the original particle boundaries. Microscopic examination of samples partially and fully reduced showed that the samples do not lose volume by shrinkage, but instead voids are created. Therefore, after the increase in particle volume brought on by the first oxidation, the second reduction should leave iron particles which are now larger and more porous than those created by the first reduction. The increased porosity (and exposed surface area) of the particles, then, is the reason that the second oxidations take place with a higher rate than the first and reach a higher asymptote as well. The observation of asymptotic oxidation behaviour at levels less than 100% conversion is believed to be due to unreacted iron and magnetite (Fe_3O_4) being trapped in the interior of the particles by the growing oxide.

4.4. X-ray diffraction and microstructural analyses

Direct evidence of the eutectoid decomposition during reduction was obtained through the X-ray diffraction experiments. Not only did these analyses show that wustite was decomposing, it also indicated that the Fe_3O_4 produced by the decomposition was preferentially reduced. A surprising result of the diffraction measurements was that the decomposition took place much faster than previously reported. The samples which were heated to temperatures below the reduction temperature and either cooled or held there contained large amounts of Fe_3O_4. It is estimated that between 10 and 15% of the wustite present decomposed in the first experiment in which the sample was heated to 598 K at 10 K min^{-1} and then immediately cooled. In the second experiment wherein the sample was heated to 598 K, then cooled to 553 K and held there for 3.5 h, an estimated 20% decomposition took place. These values are much higher than those predicted in the literature. For example, in the reported transformation curve [12], no Fe_3O_4 should be detected even after 24 h at 553 K.

5. Conclusion

The reduction of FeO powders in a hydrogen atmosphere showed a dependence on temperature relative to an effective eutectoid decomposition temperature of 803 K. Above this temperature, the reduction process is relatively slow and is limited by the direct reduction of FeO to iron. In contrast, below 803 K the reduction is relatively rapid, aided by the eutectoid decomposition of FeO to iron plus Fe_3O_4. The latter is believed to enhance the reduction by providing nucleating sites for iron and by the fact that the reduction of Fe_3O_4 is faster than that of FeO. The activation energies for reduction above and below the effective eutectoid temperature (803 K) were determined to be 51 and 58 kJ mol^{-1}, respectively. Subsequent oxidation, in air, of the iron resulting from the reduction of FeO produced, as expected, Fe_3O_4 and Fe_2O_3.

Acknowledgement

We are grateful for the financial support of this work by the Office of Basic Energy Sciences of the US Department of Energy.

References

1. A. MUAN and E. F. OSBORN, "Phase Equilibria Among Oxides in Steelmaking" (Addison-Wesley, Reading, Massachusetts, 1965) pp. 24–31.
2. E. A. GULBRANSEN and J. W. HICKMAN, *Trans. AIME* **171** (1947) 306.
3. E. T. TURKDOGAN and J. V. VINTERS, *Met. Trans.* **3** (1972) 1561.
4. S. K. EL-RAHAIBY and Y. K. RAO, *Met. Trans. B* **10B** (1979) 257.
5. J. FEINMAN and T. D. DREXLER, *AIChE J.* **7** (1986) 584.
6. M. SASABE, K. GOTO and M. SOMENO, *Trans. Iron Steel Inst. Jpn* **10** (1970) 25.
7. Z. A. MUNIR and P. G. COOMBS, *Met. Trans. B* **14B** (1983) 95.
8. P. G. COOMBS and Z. A. MUNIR, in "Precious Metals: Mining, Extraction, and Processing" edited by V. Kudryk, D. A. Corrigan and W. W. Liang (TMS-AIME, Warrendale, Pennsylvania, 1984) p. 567.
9. B. J. ASIRVATHAM and Z. A. MUNIR, *J. Mater. Sci.* **21** (1986) 1997.
10. Z. A. MUNIR and B. J. ASIRVATHAM, *ibid.* **21** (1986) 2002.
11. P. G. COOMBS and Z. A. MUNIR, *ibid.* **24** (1989) 3913.
12. M. H. DAVIES, M. T. SIMNAD and C. E. BIRCHENALL, *Trans. AIME J. Metals* **3** (1951) 889.

Received 8 June
and accepted 9 November 1988